

Effects of boron number per unit volume on the shielding properties of composites made with boron ores from China

LI Zhefu^{1,2} XUE Xiangxin^{1,2,*} LIU Sulan^{1,2} LI Yong^{1,2} DUAN Peining^{1,2}

¹School of Materials & Metallurgy, Northeastern University, Shenyang 110004, China

²Liaoning Key Laboratory for Ecologically Comprehensive Utilization of Boron Resources and Materials, Shenyang 110004, China

Abstract The total macroscopic removal cross sections, deposited energies and the absorbed doses of three new shielding composites loaded with specific boron-rich slag, boron concentrate ore and boron mud of China for ^{252}Cf neutron source were investigated by experimental and Monte Carlo calculation. The results were evaluated by boron mole numbers per unit volume in composites. The half value layers of the composites were calculated and compared with that of Portland concrete, indicating that ascending boron mole numbers per unit volume in the composites can enhance the shielding properties of the composites for ^{252}Cf neutron source.

Key words Boron ores from China, Boron mole number, Fast neutron shielding property, Monte Carlo method, Half value layers

1 Introduction

Boron, an important element used in thermal neutron shielding, is widely used in nuclear industry due to its large absorbing cross section with low energy of secondary emitted gamma rays. Several studies on shielding materials prepared using boron compounds as neutron absorbers have recently been undertaken [1–11]. However, while the neutron shielding capabilities are exceptional, all the neutron absorbers are artificial, thus limiting application of these boron compounds due to their high cost.

Many boron ore depositions have been discovered around the world, and boron as compound exists. They are more practical and cheaper than artificial boron compounds. The mixture of boron ores and hydrogen rich matrix is an effective way of shielding fast neutron. Therefore, boron-containing shielding composites for thermal neutron have the potential to shield fast neutron. Many shielding materials in Turkey are mainly prepared by using boron ores as neutron absorbers and fast neutron removal cross sections were also calculated^[1,12–17]. In

China, green boron ores mainly includes szaibelyite and ludwigite^[18]. The boron ore generated from ludwigite contains iron ore and boron concentrate ore, boron rich slag and boron mud. Compared with artificial boron compound, the green boron ore are quite abundant and of low cost. In recent years, neutron and photon shielding composites were prepared by green or artificial boron ores in China^[19–23]. To date, however, the properties of such composites in ^{252}Cf neutron shielding have not been reported to extend its application in China.

In this paper, the total fast neutron macroscopic removal cross sections of composites against a ^{252}Cf neutron source are experimentally measured. The composites are prepared using heat resistant polyimide as matrix resin, and loaded by specific boron rich slag, boron concentrate ore or boron mud from China. The deposited energies and the absorbed doses by neutron interactions with composites are calculated using the Monte-Carlo method^[12]. Experimental and calculation results are evaluated in boron mole numbers per unit volume. The half value layers of the composites were compared with that of Portland concrete.

Supported by National Natural Science Foundation of China (Grant Number: 50774022)

* Corresponding author. E-mail address: lzfneu@163.com

Received date: 2012-02-22

2 Experimental

2.1 Materials

The equipments include a wavelength dispersive spectrometer (Rigaku ZSX-100e with Rhodium target X-ray controlled by a Software ZSX computer), heat presser (20 t) and sieves.

The analysis result by the spectrometer showed the main material components (Fig.1). The chemical formula of the matrix polyimide is $C_{22}H_{10}N_2O_5$. The resin powder (1.18 g/cm^3) is measured by the pyknometer method (GB5161-85).

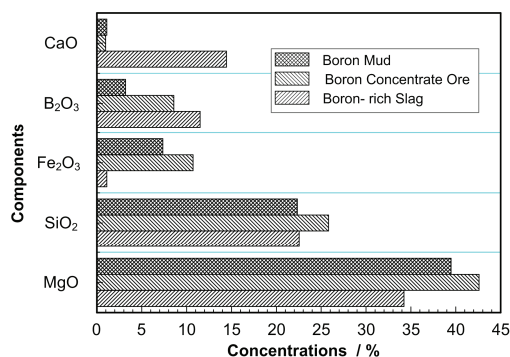


Fig.1 Element concentration (%) in oxide for different boron ores.

2.2 Samples preparation

The materials were crushed and dried in an oven at 300°C for 1 h, and sieved into about $75 \mu\text{m}$ powder. The polyimide resin as matrix is of heat resistant and

Table 1 ^{252}Cf characteristics^[24].

Neutron emission rate	$1.19 \times 10^5 \text{ n/s}\cdot\text{Bq}$
Emitted neutron number per fission	$2.34 \times 10^{12} \text{ n/s}\cdot\text{g}$
Average energy	3.76
Half life period	2.35 MeV
Half life period of Alpha decay	2.65 a
Half life period of spontaneous fission	2.73 a
Average energy of Alpha particles	85.5 a
	6.12 MeV

3 Simulations

FLUKA, an known tool to calculate particle transport and interactions with matter, can simulate the high interaction accuracy and propagation about 60 different particles, including photons of 1 keV to thousands of TeV, and neutrons down to thermal energies^[25]. The neutron cross section data were binned into 260 energy groups, where into 31 are in

radiation damage, and superfine about $15.34 \mu\text{m}$.

The materials were prepared by mixing the boron-containing ores into the 20% resin (w:w) in the agate jar, filled in the steel mold, pressed first by 5 MPa at 120°C procuring temperature for 1 h, and finally pressed by 10 MPa, at 235°C curing temperature for 1 h. Boron-rich slag, boron concentrate ore and boron mud composites were moulded into $11 \text{ cm} \times 11 \text{ cm}$ with 1.24-, 1.30- or 1.34-cm thickness, to calculate that these material densities of 2.233, 2.003, and 1.699 g/cm^3 .

2.3 Measurement

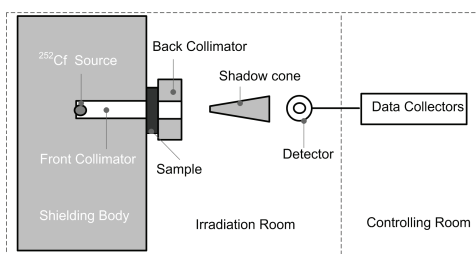
A ^{252}Cf neutron source of spontaneous fission was used, and the properties of which are listed in Tables (1) and (2). The shielding material was set between double collimators (Fig.2). The inner radius of the collimator is 10 cm and the distance from the samples to the source is 37 cm. The fast neutron detector is ^3He spherical neutron detector plus a spherical polyethylene moderator ball. The detector properties are listed in Table 3. The distance from detector to the source is 110 cm. The counting number was read from the data collectors connected to PC. The scattering neutron counting was eliminated by the shadow cone. The ambient temperature is $22\text{--}23^\circ\text{C}$, the relative humidity is 29%–31% and the atmospheric pressure is 100.8–101.1 kPa.

the thermal energy region, such as ENDF/B, JEF and JENDL were used for low energy neutron transportation below 20 MeV^[26]. Several radiation shielding studies were performed by FLUKA Monte Carlo code^[12, 27].

Here, the total macroscopic removal cross sections, absorbed doses and energies deposited by low energy neutron interactions were calculated by using the Monte Carlo code^[12].

Table 2 ^{252}Cf neutron spectra^[24].

Energy / MeV	Neutrons / s·g
0.0–0.5	2.8×10^{11}
0.5–1.0	3.7×10^{11}
1.0–2.0	7.6×10^{11}
2.0–3.0	4.6×10^{11}
3.0–4.0	2.8×10^{11}
4.0–5.0	1.6×10^{11}
5.0–6.0	5.6×10^{10}
6.0–7.0	4.0×10^{10}
7.0–8.0	1.3×10^{10}
8.0–10.0	9.9×10^9
10.0–13.0	2.2×10^9

**Fig.2** Geometrical setup of the experiment.

4 Results and Discussion

In a mixture, the total macroscopic removal cross section of a given processing interaction can be expressed as

$$\Sigma(E) = \sum_i \frac{A_v}{A_i} \rho_i \sigma_i(E) \quad (1)$$

where, A_v is the Avogadro constant, A_i is the i -th atomic weight, ρ_i is the i th atomic density in the mixture, σ_i is the i -th atomic microscopic removal cross section.

Often the total macroscopic removal cross section (Σ_t) can be calculated by adding different types of cross sections together.

$$\Sigma_t = \Sigma_s(E) + \Sigma_a(E) \quad (2)$$

The neutron attenuation relation in case of collimate narrow beam is expressed as

$$I = I_0 e^{-\Sigma_t d} \quad (3)$$

Table 3 Properties of the Detector.

Detector	^3He Proportional Counter
Moderator	Spherical Polyethylene Moderator Body
Moderator Size / mm	295 mm diameter
Detector Sensitivities	$1-10^5 \mu\text{Sv/h}$
Energy Range	$2.5 \times 10^{-8}-16 \text{ MeV}$
Operating Temperature	$0-+55^\circ\text{C}$
Working Voltage	900–1500 V

where, I is the beam intensity that penetrates through the composites, I_0 is the beam intensity in case of no shielding material exists, and d is the material thickness.

Therefore, total macroscopic removal cross section can be expressed as

$$\Sigma_t = (1/d) \ln(I_0/I) \quad (4)$$

Eq.(4) can also be expressed as

$$\ln(I_0/I) = \Sigma_t d \quad (5)$$

The relationship between half value layers of the composites and the total macroscopic removal cross section is

$$d_{1/2} = \ln 2 / \Sigma_t \quad (6)$$

The total neutron removal macroscopic cross sections have been measured by ^3He detector and calculated by the Monte Carlo method (Table 4). The average counts and the absolute deviation of background, bare source and the counts that loaded with composites were measured and calculated in the experiments. The net counts can be calculated by the difference between the average counts of bare source and background, the counts with composites and background. The macroscopic removal cross sections and their absolute deviation can be calculated by Eq.(4). Therefore, the absolute deviation of boron-rich slag, boron concentrate ore and boron mud composites were 2%, 1% and 1%, respectively.

In Fig.1 and Eq.(1), all the components in the composites are related to the macroscopic removal cross sections for fast neutron. In Table 4, the macroscopic removal cross sections increase with the

boron mole numbers of the composites. Calculations results using Eq.(4) show that the macroscopic removal cross section depends on the boron intensities of the composites.

Table 4 Boron mole numbers per unit volume and the macroscopic removal cross sections.

Boron Ores in Composites	Boron Mole Numbers per Unit Volume (mol/cm ³)	Macroscopic Removal Cross sections by FLUKA calculation (cm ⁻¹)	Experiments (cm ⁻¹)
Boron rich slag	8.1505×10^{-3}	0.2394 ± 0.00005	0.25 ± 0.02
Boron concentrate ore	5.3367×10^{-3}	0.2133 ± 0.00002	0.22 ± 0.01
Boron mud	1.7886×10^{-3}	0.1850 ± 0.00005	0.19 ± 0.01

The deposited energy per primary fast neutron of the three composites is calculated by FLUKA (Fig.3). The deposited energy increases with boron mole numbers, indicating a linear increase trend. Also, the absorbed dose for fast neutron increases with boron mole numbers per unit volume (Fig.4). The natural logarithm of the initial neutron counts relative to the transmitted one $\ln(I_0/I)$ versus composites thickness (d) are calculated (Fig.5). The linear dependence complies well with the exponential relation in Eq.(4), the values linearly increase with the composites thickness, and comply with Eq.(5). Thus, the slopes of the lines are the macroscopic removal cross sections for fast neutron with 15-cm thickness. Fig.5 shows the linear fit equations.

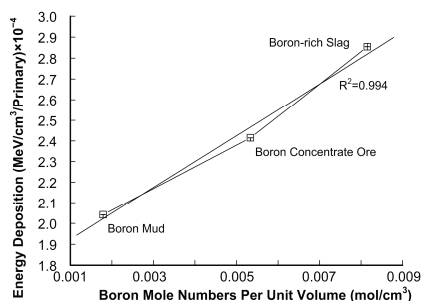


Fig.3 Energy deposition as a function of boron mole numbers per unit volume.

As a promising building material for fast neutron shielding, the half value layers of the three boron-containing ores composites were calculated and compared with that of Portland concrete^[28] according to Eq.(6) (Fig.6). The half value layer of boron-rich slag composites for fast neutron approach to that of Portland concrete; boron concentrate ore and boron mud composite are even worse. Therefore, ascending boron mole numbers per unit volume can improve the shielding properties for fast neutron.

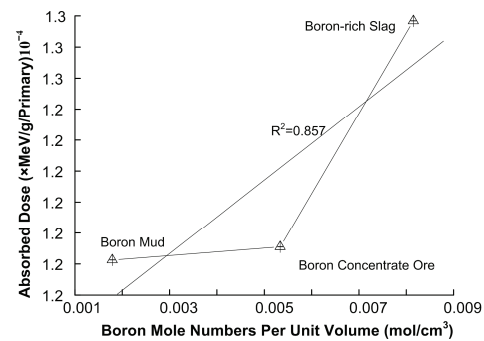


Fig.4 Absorbed dose as a function of boron mole numbers per unit volume.

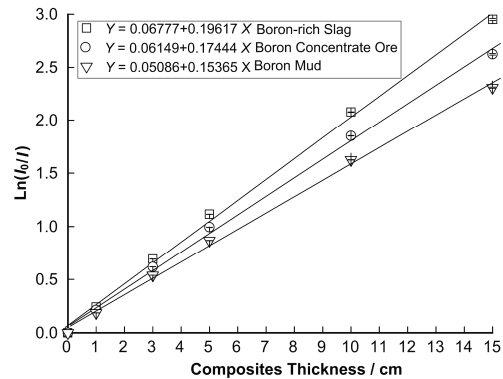


Fig.5 The variations of $\ln(I_0/I)$ with composites thickness.

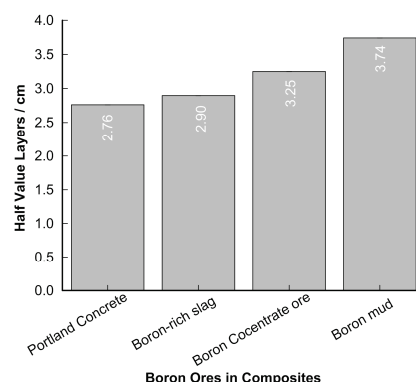


Fig.6 Half value layers of the composites.

5 Conclusions

Polyimide resin loaded with boron-rich slag, boron concentrate ore, and boron mud from China as composites were prepared, and the shielding properties of three boron-containing ores composites for fast neutrons were investigated by experiment and Monte Carlo calculation.

All the components in the composites are related to the macroscopic removal cross section and the measured and calculated macroscopic removal cross sections increase with boron mole numbers. Energy deposition and the absorbed doses of fast neutrons increase with boron mole numbers in the shielding materials. The transmission values exponentially decrease with increasing the composites thickness for the composites. The half value layers of boron-containing ores composites decrease with increasing boron mole numbers. The half value layers of boron rich slag composite approach to that of Portland concrete, and is the best in the other two boron-containing ores composites. Ascending boron mole numbers per unit volume can improve the neutron shielding properties of the composites.

References

- 1 Faruk D. Appl Radiat Isot, 2010, **68**: 175–179.
- 2 Atsuhiro M, Sukegawa, Y A, Koichi O, *et al.* J Nucl Mater, 2011, **417**: 850–853.
- 3 Hayashi T, Tobita K, Nakamori Y, *et al.* J Nucl Mater, 2009, **386–388**: 119–121.
- 4 Majid J, Ali M. Radiat Phys Chem, 2008, **77**: 523–527.
- 5 Atsuhiro M, Shinji S, Koichi O, *et al.* J Nucl Mater, 2007, **367–370**: 1085–1089.
- 6 Celli M, Grazzi F, Zoppi M. Nucl Instrum Meth Phys Res A, 2006, **565**: 861–863.
- 7 Yoshinori S, Akira S, Tooru K. Nucl Instrum Meth Phys Res Sect A, 2004, **522**: 455–461.
- 8 Atsuhiro M, Satoshi S, Masaharu K, *et al.* J Nucl Mater, 2004, **329–333**: 1619–1623.
- 9 Harvinde r S, Kulwant S, Leif G, *et al.* Nucl Instrum Meth Phys Res B, 2003, **207**: 257–262.
- 10 Gwaily S E, Hassan H H, Badawy M M, *et al.* Polym Test, 2002, **21**: 513–517.
- 11 Gwaily S E, Badawy M M, Hassan H H, *et al.* Polym Test, 2002, **21**: 129–133.
- 12 Turgay K, Abdulhalik K, Gökhan B, *et al.* Appl Radiat Isot, 2012, **70**: 341–345.
- 13 Turgay K, Adem Ü, Faruk D, *et al.* Ann Nucl Energy, 2010, **37**: 996–998.
- 14 El-Khayatt A M. Ann Nucl Energy, 2010, **37**: 218–222.
- 15 Demet D, Gürbüz K. Nucl Instrum Meth Phys Res B, 2006, **245**: 501–504.
- 16 Koichi O. Radiat Prot Dosim, 2005, **115**: 258–261.
- 17 El-Sayed Abdo A. Ann Nucl Energy, 2002, **29**: 1977–1988.
- 18 Liu S L, Cui C M, Zhang X P. ISIJ Int, 1998, **38**: 1077–1079.
- 19 Li Z F, Xue X X, Jiang T, *et al.* Adv Mater Res, 2011, **201–203**: 2767–2771.
- 20 Li Z F, Xue X X. At Energy Sci Technol, 2011, **45**: 1147–1152.
- 21 Li Z F, Xue X X. At Energy Sci Technol, 2011, **45**: 223–229.
- 22 Li Z F, Xue X X. J Northeastern Univ, 2011, **32**: 1716–1720.
- 23 Li Z F, Xue X X, Jiang T. J Funct Mater, 2010, **41**: 1892–1895.
- 24 Edward Profio A. Radiation shielding and dosimetry. United States: John Wiley & Sons, Inc, 1979, 13.
- 25 Ferrari A, Sala P R, Fassò A, *et al.* CERN-2005-10 (2005), INFN/TC_05/11, SLAC-R-773.
- 26 Giuseppe B, Francesco B, Markus B, *et al.* Nucl Instrum Meth Phys Res Sect B, 2011, **269**: 2850–2856.
- 27 Turgay K, Hatun K, Abdulhalik K, *et al.* Ann Nucl Energy, 2011, **38**: 56–59.
- 28 İbrahim T, Yüksel Ö, Murat K, *et al.* Ann Nucl Energy, 2008, **35**: 1937–1943.